Influence of alkaline pre-treatment on acid dissolution of cathode material of 18650 lithium battery

Influence of alkaline pre-treatment on acid dissolution of cathode material of 18650 lithium battery

Dessy Amalia[1], Pritam Singh[1], Wensheng Zhang[2] and Aleksandar N. Nikoloski[1*]

[1]Harry Butler Institute (Centre for Water Energy and Waste), Engineering and Energy, Murdoch University, 90 South Street, Murdoch, 6150, Western Australia, Australia
[2]CSIRO Mineral Resources, PO Box 7229, Karawara, WA 6152, Australia

*Corresponding author's e-mail: A.Nikoloski@murdoch.edu.au

Abstract: Lithium battery cathodes contain lithium, cobalt, nickel, and manganese. Recycling of spent lithium batteries aims to recover these elements for re-use. Liberation of cathode materials from other metals in the battery such as aluminium, copper, and iron, is essential to obtain a good leaching efficiency in the recovery of valuable metals from end-of-life lithium batteries. This study investigates the behaviour of cathode materials and other metals in spent 18650 lithium batteries during leaching in H_2SO_4 solution with and without NaOH pre-treatment. Dissolution of aluminium using NaOH is a selective method to separate the metal from other elements. The influence of a 2-hour NaOH pre-treatment on subsequent acid leaching of cathode materials was investigated at both room temperature and 80°C. The extraction of aluminium increased to 75% at a higher temperature. Lithium concentration in the pregnant leach solution from acid leaching also increases with NaOH pre-treatment. The pre-treatment had a negligible effect on nickel, manganese, iron, and copper extraction. However, the cobalt extraction with NaOH pre-treatment was significantly lower. The result was likely due to indirect impact of less hydrogen gas was generated from a lower Al amount. The lattice structure of the leach residue for the sample with NaOH pre-treatment was monoclinic rather than rhombohedral due to stronger delithiation.

1. Introduction

Lithium batteries are increasingly being used in many applications both for electronic devices and energy storage. The development of an efficient recycling system is essential to recover the valuable elements in these batteries for sustainable use of material resources [1,2]. Both pyrometallurgy and hydrometallurgy are used in lithium battery recycling to extract the metals of the cathode material. Some commercial plants use pyrometallurgy to treat the spent batteries using smelting furnaces. The process removes the need for mechanical treatment, as it burns most of the battery outer casing, carbon, and plastic separator. The high-temperature treatment produces alloys of cobalt (Co), copper (Cu), nickel (Ni), and polymetallic slags of aluminium (Al), lithium (Li), and iron (Fe) [3]. A further process is required to recover Li from the slag with hydrometallurgy, but the process consumes a lot of energy [4] Thus, hydrometallurgy is increasingly being investigated for use in lithium battery recycling.

The 18650 lithium batteries have a layered structure of cathode and anode materials with a polymeric separator in between. The material is rolled and then wrapped in a stainless-steel casing. Cathode materials containing lithium metal oxide nanoparticles are attached to aluminium foil by a

polyvinylidene fluoride (PVDF) binder and the foil serves as the current collector. Because of this structure, it is necessary to detach the Al foil from the cathodes materials as part of the process to recover the valuable metals. Large-scale plants use mechanical treatment to separate metals (Fe, Cu, and Al) from the cathode materials, but the product still contains 3 - 5wt% Al at particle sizes ranging from 2000 – 250 μm [5]. This aluminium consumes acid during the leaching process, so the removal of aluminium prior to the leaching is desirable.

Methods to separate Al from the cathode materials include removing the PVDF by heating at 300 - 600°C or dissolving it using N-methyl-2-pyrrolidone (NMP) [6–9]. However, the heating treatment generates a poisonous and hazardous gas, HF, due to PVDF decomposition [10,11], and the NMP is volatile, flammable, explosive, toxic, and expensive [10–13]. An alternative is leaching the battery material in NaOH to selectively separate Al from the other elements. Most reports of the application of NaOH leaching for Al removal include a prior process where operators manually dismantle the battery before processing the cathode metals [6,14–16].

This study aimed to understand the behaviour of elements in the cathode materials and other metals (Cu, Al, and Fe) in spent lithium-ion batteries during acid leaching with and without alkaline pre-treatment. Phase changes of the cathode materials were examined to establish the likely reactions taking place during the process. This study did not include the effect of reductant addition to investigating the influence of the impurity elements (Cu, Fe, Al) on the dissolution of the cathode materials after the pre-treatment, which has not been reported in previous studies.

2. Experimental

2.1. Materials and reagents

Spent lithium-ion batteries (LIBs) from laptop computers were obtained from Total Green Recycling, Australia. The batteries were from different manufacturers and varied in composition.

The chemical reagents used in these experiments were sodium hydroxide (NaOH) for pre-treatment and sulphuric acid (H_2SO_4) for acid leaching. The digestion for elemental analysis of the feed material used aqua regia, which was a mixture of nitric acid (HNO_3) and hydrochloric acid (HCl) in the ratio 1:3. All reagents were of analytical grade from UNIVAR (Ajax Finechem) and were used as received without further purification.

2.2. Discharging and mechanical treatment

Each spent laptop battery was immersed in a NaOH solution (7 wt%) for 24 hours and the outer polymer casing was then manually removed to free the cylindrical 18650 batteries. The batteries were further discharged in the same alkaline solution for 24 hours. The discharged batteries were shredded using a cutting mill Retsch SM200. The milled materials contained cathode materials of the primary target metals (Li, Co, Mn, Ni), carbon, and few associated metals (Fe, Al, Cu) after sieving it with a 180-μm screen. The sieved particles of sizes smaller than 180 μm were used in the leaching tests.

2.3. Leaching tests

Direct acid leaching and NaOH treatment before acid leaching were used in these tests. The direct acid leaching was conducted at two temperatures, 40 and 85°C. The leaching used 2M H_2SO_4 with a solid/liquid ratio of 100 g/L. The sample was leached in a 250-ml three-neck round-bottom glass reactor for 4 hours. The slurry was stirred at 400 rpm using a magnetic bar stirrer. The reactor was placed in an oil bath to control the temperature and connected to a condenser to reduce the water evaporation. During the leaching process, 1 ml of the aqueous solution was extracted at specified times for elemental analysis after dilution and syringe filtration. The slurry was filtered at the end of the test to separate the leachate and the residue. The pregnant leach solution (PLS) for the test at 85°C (sample SA-1) was analysed for chemical composition.

The aim of pre-treatment test before leaching was to extract Al selectively from other metals. The pre-treatment used a 2M NaOH with a slurry density of 100 g/L. The tests were conducted at room

temperature and 80°C. The slurry was placed in a glass reactor for 2 hours and at the end of the test, the slurry was filtered to obtain the undissolved material. The residue of the test at 80°C was washed and dried before undergoing acid leaching. The acid leaching was performed using the same conditions as direct acid leaching at 85°C. The PLS of the process was termed sample SA-2.

2.4. Analyses

The mineral composition of the feed (-180 μm sample) and the solid leach residue were examined qualitatively using an X-Ray diffractometer (XRD CuKα - GBC Emma). The quantitative analysis of the Al, Fe, Cu, Mn, Ni, Co, and Li content in the leachate and digested solid solutions was performed using ICP-OES (Thermo Fisher Scientific iCAP 7600 Duo). The surface morphology study and trace elements were conducted by using an ultrahighresolution SEM, tescan Clara. Carbon content was measured using Thermo scientific EA isolink without IRMS. The solid samples of the feed were digested using aqua regia and dissolved in HCl.

The metal extraction as a function of time was calculated by comparing the extracted metal weight in the solution at a particular time (W_t) to the initial weight (W_i) of the sample (equation 1).

$$\% \text{ element extraction} = \frac{W_t}{W_i}\, x\, 100\% \quad (1)$$

3. Results and discussion

The Rietveld refinement of the XRD spectra for the feed contains features corresponding to the cathode materials in the sample, lithium cobalt oxide (LCO), lithium nickel manganese cobalt oxide (NMC), and lithium manganese oxide (Li_2MnO_3). The elemental composition of the feed in table 1 shows that cobalt is the dominant metal of interest in the sample, contributing to the primary cathode type of LCO. The associated metals (Al, Fe, and Cu) account for less than 2.0 wt.-%. The remaining components in the sample were carbon (31.26%) from the anode, electrode, and trace elements which were detected by SEM EDS mapping.

Table 1. Concentration of the key elements in the feed sample.

Element	Al	Fe	Cu	Co	Ni	Mn	Li
Wt.-%	1.60	1.27	1.02	26.69	3.88	2.68	4.19

3.1. Direct acid leaching

Figures 1 (a) and (b) show that aluminium dissolution in direct acid leaching was not greatly affected by temperature and ranged from 80-90% in the tests at both 40 and 85°C, reaching the maximum extent of dissolution in less than an hour. Aluminium metal is more reactive than Fe and Cu as its standard reduction potential is more negative (table 2) and it therefore easily oxidises in the H_2SO_4 solution via (reaction 2) below. The undissolved Al can be partly related to aluminium oxide (Al_2O_3) and aluminium silicate, which were detected in the residue using SEM EDS (figure 2). The aluminium oxide in the material is from the surface coating on the electrode, which is used to stabilise the electrode-electrolyte interface [17]. This oxide is chemically stable and has a slow dissolution rate (reaction 3) even in a highly concentrated sulphuric acid solution above 100°C [18]. The trace aluminium silicate is possibly a leftover impurity that was contained in the aluminium ore, bauxite [19]. The Si content in Al cathode foil in the market ranges from 0.2 to 0.25% [20–22].

$$2Al\,(s) + 3H_2SO_4\,(aq) = Al_2(SO_4)_3\,(aq) + 3H_2\,(g)\quad \Delta G°_{298} = -969.928\ kJ) \quad (2)$$

$$Al_2O_3 + 3H_2SO_4\,(aq) = Al_2(SO_4)_3\,(aq) + 3H_2O\,(aq)\ (\Delta G°_{303} = -259.910\ kJ) \quad (3)$$

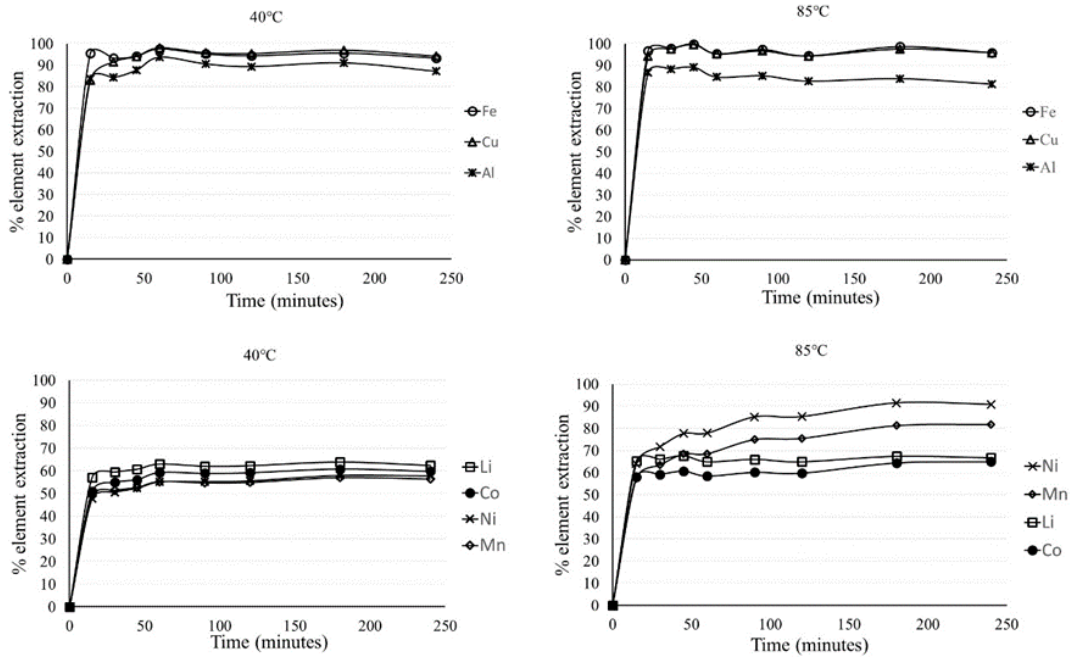

Figure 1. Extractive yields of different elements versus time during direct acid leaching in 2M H_2SO_4 at 40°C (a, c) for Al, Cu and Fe; and 85°C (b, d) for Co, Ni, Li and Mn.

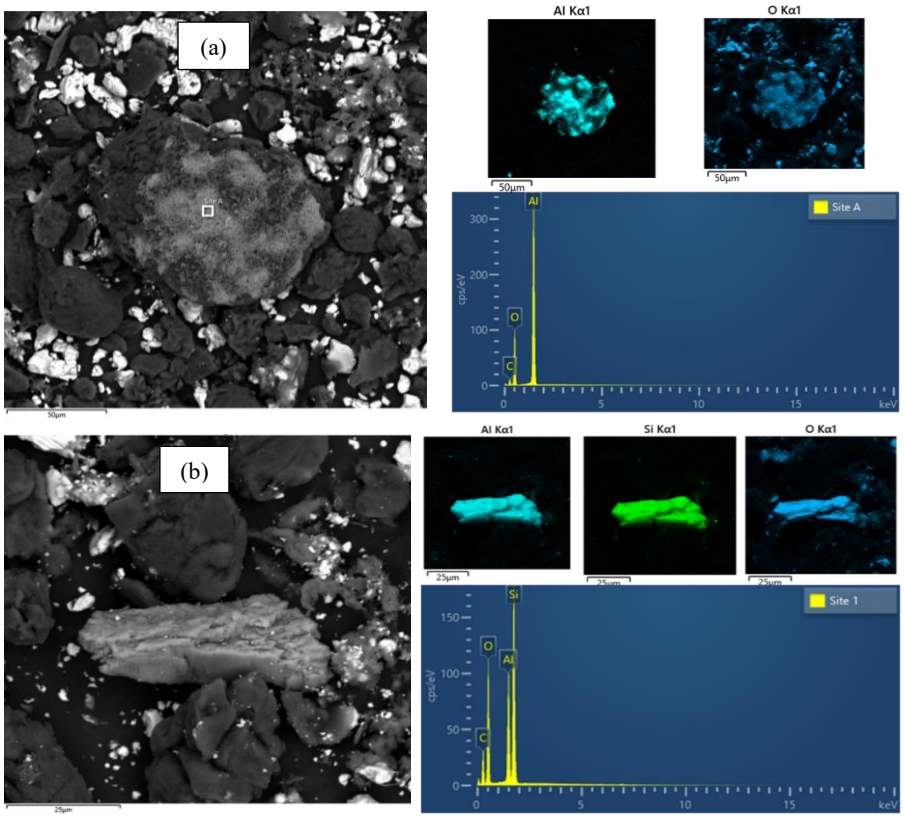

Figure 2. SEM EDS Mapping of a) aluminium oxide and b) aluminium-silicate in the residue after leaching in H_2SO_4 solution.

The dissolution of Fe and Cu in the acid solution was also not significantly affected by the temperature increase, reaching over 95% in less than an hour in both cases, as seen in figures 1a and 1b. According to the standard reduction potentials in table 2, Fe metal will dissolve in the H_2SO_4 solution, but the dissolution of copper metal can only occur in the presence of an oxidant or through the catalytic action of a ferric ion.

Table 2. List of standard reduction potentials relative to a hydrogen electrode (SHE) for relevant reactions in the study [23]

Reaction	$E°_{298}$ (volt)
$O_2 + 4H^+ + 4e^- = 2H_2O$	1.23
$Fe^{3+} + 2e^- = Fe^{2+}$	0.771
$O_2(g) + 2H_2O + 4e^- = 4OH^-$	0.401
$Cu^{2+} + 2e^- = Cu(s)$	0.339
$Fe^{2+} + 2e^- = Fe(s)$	-0.44
$Al^{3+} + 3e^- = Al(s)$	-1.677
$Al(OH)_4^- + 3e^- = Al(s) + 3OH^-$	-2.328

The proposed reaction of LCO with sulphuric acid in equation 4 generates oxygen [24,25], which possibly affects the copper oxidation. The iron oxidation to Fe^{2+} was higher at the beginning of the experiment (after 15 minutes) than Cu oxidation. The ferrous ion may act as a reductant for lithium cobalt oxide (LCO) and converted to ferric. The possible reaction in sulphuric acid is shown below (equation 5). Another possible reductant for the LCO is copper with Fe(II)/Fe(III) as a redox catalyst in equation 6 [26]. The increased copper dissolution at 85°C (figure 1.b) since the first 15 minutes of reaction as ferrous iron shows that the reduction process by Cu was favoured at high temperatures. The Co extraction apparently also rose up at the same time (figure 1.d). The generation of hydrogen gas from aluminium dissolution (equation 2) also can contribute to the reduction of LCO.

$$4\,LiCoO_2\,(s) + 6\,H_2SO_4 \rightarrow 4\,CoSO_4\,(aq) + 2\,Li_2SO_4\,(aq) + 6H_2O + O_2\,(g) \quad (4)$$

$$Fe^{2+} + LiCoO_2 + 4\,H^+ \rightarrow Li^+ + Co^{2+} + Fe^{3+} + 2\,H_2O \qquad (\Delta G = -145.467\ kJ) \quad (5)$$

$$2LiCoO_2 + Cu + 8H^+ \xrightarrow{Fe(II)/Fe(III)} 2Li^+ + 2Co^{2+} + 4H_2O + Cu^{2+} \quad (6)$$

Lithium extraction was higher than that of cobalt at both temperatures. The c/a lattice value (table 3) of the LCO peak in the feed is 4.99, which is characteristic of high temperature (HT) LCO [27]. The HT-LCO has a hexagonal structure where Li is located between octahedral layers of cobalt and oxygen. The Co-O has a strong covalent bond (Chapter 5 of [28]). The interaction between a single-state metal ion layer and oxygen is not as strong as the metal-oxygen bond [29]. This property leads to delithiation during the charging-discharging process, which follows reaction 7 [30].

$$LiCoO_2 + C_6 = Li_{(1-x)}CoO_2 + LixC_6 \quad (7)$$

The acid leaching has the same impact on lithium as it is oxidised by hydrogen ions (H^+). The oxidation reaction which dissolved the Li is believed to have transformed the LCO phase to a $Li_{0.6}CoO_2$ form which was detected in the residue, based on the diffraction spectra obtained by XRD analysis. The phase has a decreased metal-metal intra-layer distance (a) and an increased inter-slab distance (c) as reported in Table 3. The result suggests that partial delithiation from the LCO enlarges the adjacent oxygen sheets due to oxygen vacancies, leading to disproportionation of Co^{3+} to Co^{2+} and Co^{4+} [29,31].

The change of the lattice parameter c in the residue supports the occurrence of reaction 4, in which the oxidation of LCO leads to released oxygen. The reaction will have lasted when the acid-resistant cobalt oxide was formed [16].

A significant increase in extraction of Ni (from 60 to 90%) and Mn (from 60 to 80%) was observed with the increase in temperature, with both metals reaching maximum extraction after approximately 3 hours. The results are shown in figure 1c and figure1d. Disproportionation is believed to occur in Mn and Ni during delithiation. The Li extraction is believed to be related to the oxidation of Ni and Mn to the tetravalent oxidation state, with the higher state of charge and higher temperature favouring proton exchanges [26] and increasing the Mn and Ni dissolution. However, the NiO phase, in general, is less stable, which may explain the higher dissolution of Ni than Mn.

The observed increase in the extraction of Ni and Mn by approximately 6% after 2 hours may also be related to the disproportionation of Co^{3+} from the NCM material to Co^{2+}. This is supported by a slight increase in cobalt extraction of 5% after 2 hours. However, the effect is relatively small, and Co would require a reductant for higher extraction to be achieved in the acid system.

3.2. Alkaline pre-treatment before acid leaching

A study has reported that Al should be removed before the acid leaching to avoid the co-extraction of Al during Co and Cu separation [24]. Al extraction in NaOH solution is recommended as a selective leaching system. Figure 3 shows that during the NaOH pre-treatment, Al dissolved moderately at room temperature with dissolution reaching 60% after about 50 minutes. The process is spontaneous even at room temperature (reaction 8). At the higher temperature of 80°C, the dissolution of Al increased to a maximum of 75% but this was obtained after only a few minutes. Exfoliated aluminium silicate was detected using SEM EDS (figure 4) which presumably is a result of Al dissolution from the feed. The undissolved Al was from Al oxide and aluminium silicate, although this material is reactive in concentrated NaOH at high temperatures [32].

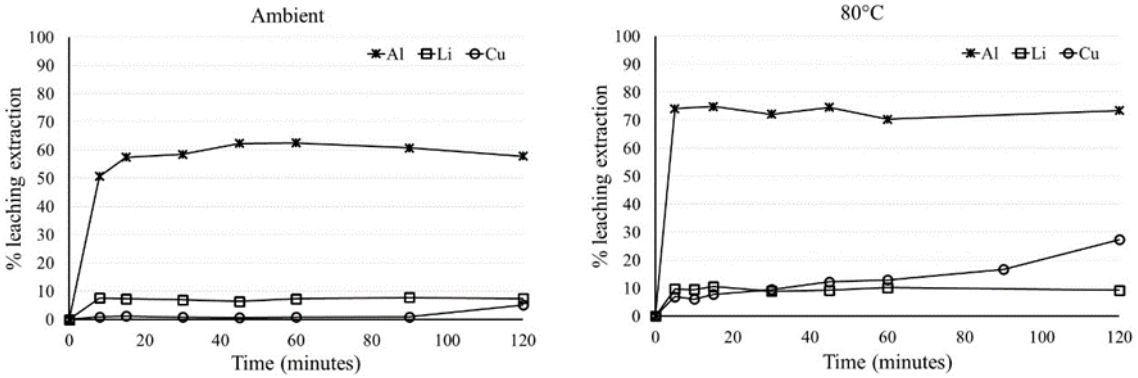

Figure 3. Profiles of Al and Li dissolution during the NaOH pre-treatment of the sample at room temperature and 80ºC.

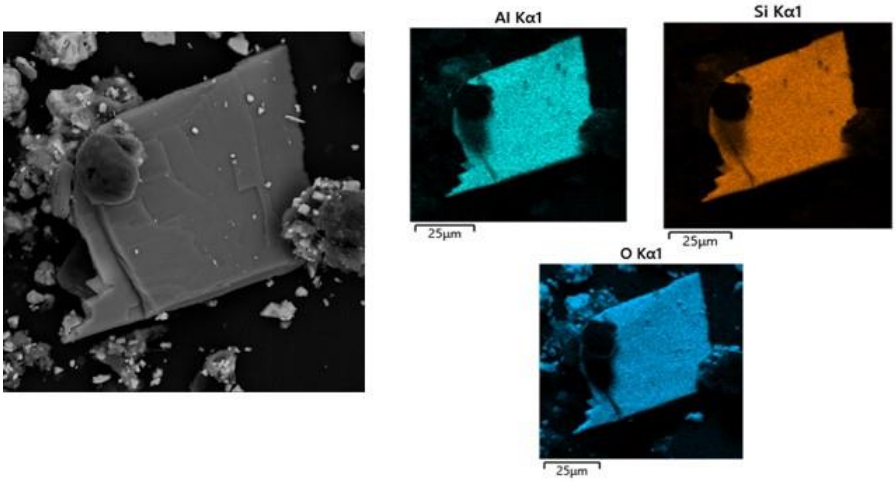

Figure 4. Exfoliated aluminium silicate in the residue of alkaline pre-treatment.

The data in figure 3 shows that the extent of dissolution of Li was not significantly affected by temperature. The Li extraction was possibly from the electrolyte ($LiPF_6$) as LCO is stable in alkaline solution [16]. Copper was detected in the PLS due to oxidation by oxygen generated from hydroxyl ion oxidation. Halliday [33] states that copper oxidation produces an oxide film on the particle surface which transforms to $Cu(OH)_2$. The hydroxides are removed from the surface into the solution due to stirring.

$$Al + NaOH\ (s) + 3H_2O\ (l) = NaAl(OH)_4\ (a) + 1.5H_2(g)\ (\Delta G^\circ_{303} = -476.780\ kJ) \quad (8)$$

Alkaline pre-treatment did not result in a significant change in the Ni, Mn, Fe, and Cu extraction extents or rates during subsequent acid leaching. Figure 5 shows that Cu dissolution was over 90% in the acid, which could be related to the oxygen generation from the delithiation process discussed earlier. The Ni and Mn also displayed a similar leaching extraction behaviour as obtained during the direct acid leaching (figure 1.b). The Ni and Mn were apparently only influenced by the leaching temperature. Similar results have been reported earlier for leaching NMC material in sulphuric acid [34].

Alkaline pre-treatment benefits the lithium recovery as the extraction of lithium from the pre-treated material increased by about 10% compared to the untreated sample. The pre-treatment is likely to have exposed a larger surface of the cathode materials due to Al detachment. The NaOH likely reacted with the binder (PVDF) which reduced the mechanical strength of PVDF, especially at the higher temperature [35].

The Li dissolution in the acid transformed the surface of the LCO to a honeycomb structure as phase form changed, as shown in figure 6. The XRD spectra comparison of the acid leaching feed and residues in figure 6 shows the transformation of LCO material. The crystal surface on the residue with alkaline pre-treatment (SA-2) was detected as the $Li_{0.5}CoO_2$ (figure 6.c) phase which has a monoclinic structure. The lower c parameter value (table 3) of the phase means the Li ordering sheared the rhombohedral oxygen lattice [27], which led to decreased charge on the oxide and the formation of oxygen vacancies [31,36].

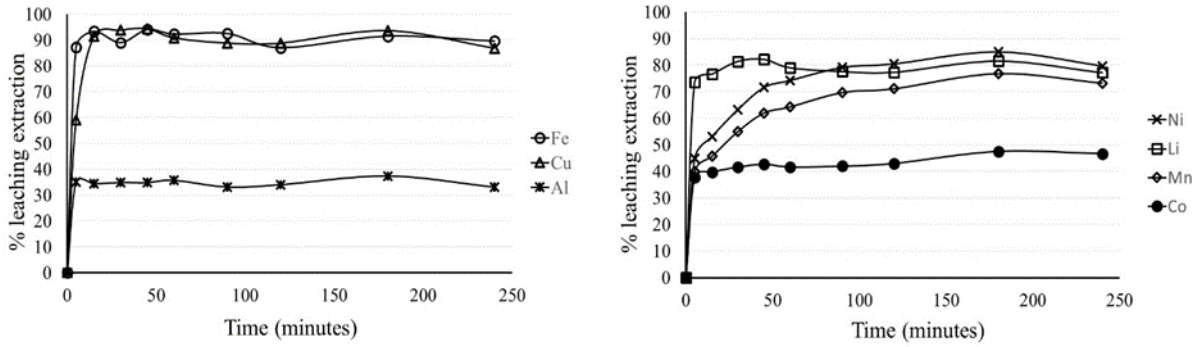

Figure 5. Element extraction profile of a) Fe, Cu, Al, and b) Ni, Mn, Li, Co, during acid leaching at 85°C for 4 hours.

The Co extraction in the acid leaching after the alkaline pre-treatment was 40-45% which is lower than direct acid leaching (60-65%). The Ni and Mn extractions were 85% and 75 % respectively, which is less than 5% each than direct acid leaching. The lower Co extraction could be attributed to the instability of LCO structure due to a higher oxygen loss in deep delithiation [37]. The O vacancy changed the Co-O bond structure and adjusted the charge distribution. Both impacted the disproportion of Co^{3+} to a higher oxidation state around the O vacancy [38], meaning the Co would require more reductant in the leaching system of the pre-treated material than in the direct acid leaching process. The result appears to suggest the significantly low amount of Al after the pre-treatment (table 4) was indirectly affected the reduction process of cathode materials. The absence of hydrogen gas from Al dissolution impacted to the less reductive environment of the acid leaching. The effect contributed to significantly decreased the Co extraction by 20% after the pre-treatment.

The concentration of the key elements in the PLS produced in direct leaching (SA-1) and in acid leaching with pre-treatment in NaOH (SA-2) are given in table 4. The relatively lower concentration of Al in SA-2 compared to SA-1 and the relatively higher or similar concentrations of the other elements in the PLS demonstrate the selectivity of NaOH pre-treatment for Al removal. The alkaline pre-treatment solution may be re-used after the Al is precipitated by Al_2O_3 seed.

Table 3. Comparison of LCO structure and lattice of feed and residues

Sample	Crystal system	Space group	Lattice	a	b	c
Feed	Hexagonal	R-3m	(003)	2.817	2.817	14.065
SA-1	Hexagonal	R-3m	(003)	2.8090	2.8090	14.3890
SA-2	Monoclinic	P ½ m 1	(001)	4.8650	2.8090	5.063

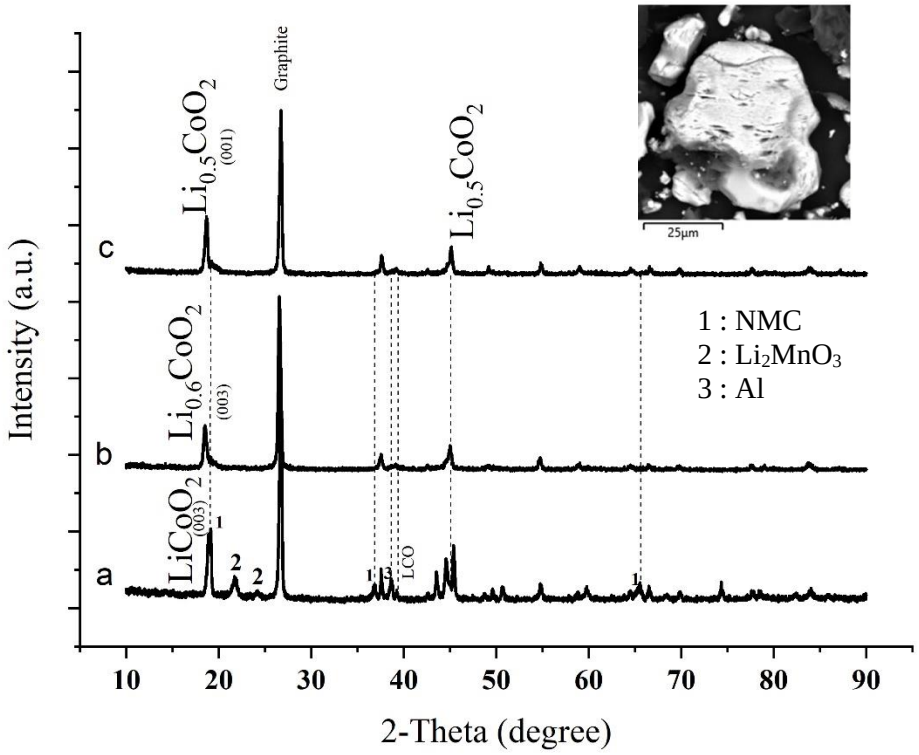

Figure 6. XRD spectra of feed (a) and residues from acid leaching without NaOH pre-treatment (b) and after NaOH pre-treatment (c) with the morphology of LCO after acid leaching.

Table 4. Element concentration (g/L) in the leachate after leaching in H_2SO_4 2 M at 85°C for 4 hours without (SA-1) and with NaOH pre-treatment (SA-2).

Sample	Element Concentration (g/L)						
	Al	Fe	Ni	Cu	Mn	Li	Co
SA-1	1.30	1.44	4.15	1.15	2.59	3.16	19.69
SA-2	0.20	1.54	5.11	1.06	3.46	3.97	18.25

4. Conclusions

The study has shown that alkaline pre-treatment dissolves Al selectively from the cathode materials. The alkaline solution also weakened the mechanical binding of PVDF which improved the liberation of the cathode materials. However, the pre-treatment also dissolved small amounts of copper as it was oxidised by the hydroxyl ion. The co-extraction reduced the copper concentration in the PLS of acid leaching.

This study further showed that the alkaline pre-treatment for Al removal before acid leaching increased Li extraction in the subsequent acid leaching by 10%. The alkaline pre-treatment had a negligible impact on the extractions of Ni, Mn, and Cu. The Ni and Mn extractions in the acid leaching of pre-treated material were only affected by an increase in temperature.

However, the extent of cobalt dissolution in the acid decreased after the alkaline pre-treatment, possibly due to the reduced amount of aluminium which was indirectly impacted the reduction of

cathode materials. This may indicate a need to increase the reductant dosage in the subsequent acid leaching to be more effectively dissolving the cobalt after alkaline treatment.

References

[1] Greim P, Solomon A A and Breyer C 2020 Assessment of lithium criticality in the global energy transition and addressing policy gaps in transportation *Nat. Commun.* **11** 4570
[2] Xu C, Dai Q, Gaines L, Hu M, Tukker A and Steubing B 2020 Future material demand for automotive lithium-based batteries *Commun. Mater.* **1** 99
[3] Mansur M B, Guimarães A S and Petraniková M 2021 An overview on the recovery of cobalt from end-of-life lithium ion batteries *Miner. Process. Extr. Metall. Rev.* 1–21
[4] Liu C, Lin J, Cao H, Zhang Y and Sun Z 2019 Recycling of spent lithium-ion batteries in view of lithium recovery: A critical review *J. Clean. Prod.* **228** 801–13
[5] Peng F, Mu D, Li R, Liu Y, Ji Y, Dai C and Ding F 2019 Impurity removal with highly selective and efficient methods and the recycling of transition metals from spent lithium-ion batteries *RSC Adv.* **9** 21922–30
[6] Meshram P, Pandey B D and Mankhand T R 2015 Hydrometallurgical processing of spent lithium ion batteries (LIBs) in the presence of a reducing agent with emphasis on kinetics of leaching *Chem. Eng. J.* **281** 418–27
[7] Liu K and Zhang F S 2016 Innovative leaching of cobalt and lithium from spent lithium-ion batteries and simultaneous dechlorination of polyvinyl chloride in subcritical water *J. Hazard. Mater.* **316** 19–25
[8] Nayaka G P, Pai K V, Manjanna J and Keny S J 2016 Use of mild organic acid reagents to recover the Co and Li from spent Li-ion batteries *Waste Manag.* **51** 234–8
[9] Chen X, Ma H, Luo C and Zhou T 2017 Recovery of valuable metals from waste cathode materials of spent lithium-ion batteries using mild phosphoric acid *J. Hazard. Mater.* **326** 77–86
[10] Lv W, Wang Z, Cao H, Sun Y, Zhang Y and Sun Z 2018 A critical review and analysis on the recycling of spent lithium-ion batteries *ACS Sustain. Chem. Eng.* **6** 1504–21
[11] Zheng X, Zhu Z, Lin X, Zhang Y, He Y, Cao H and Sun Z 2018 A mini-review on metal recycling from spent lithium ion batteries *Engineering* **4** 361–70
[12] Li J-T, Wu Z-Y, Lu Y-Q, Yao-Zhou, Huang Q, Huang L and Sun S-G 2017 2017 Water soluble binder, an electrochemical performance booster for electrode material with high Energy Density.pdf *Adv. Energy Mater.* **7** 1–30
[13] Liu X, Li D, Bai S and Zhou H 2015 Promotional recyclable Li-ion batteries by a magnetic binder with anti-vibration and non-fatigue performance *J. Mater. Chem. A* **3** 15403–7
[14] Tanong K, Coudert L, Mercier G and Blais J-F 2016 Recovery of metals from a mixture of various spent batteries by a hydrometallurgical process *J. Environ. Manage.* **181** 95–107
[15] Chen L, Tang X, Zhang Y, Li L, Zeng Z and Zhang Y 2011 Process for the recovery of cobalt oxalate from spent lithium-ion batteries *Hydrometallurgy* **108** 80–6
[16] Ferreira D A, Prados L M Z, Majuste D and Mansur M B 2009 Hydrometallurgical separation of aluminium, cobalt, copper and lithium from spent Li-ion batteries *J. Power Sources* **187** 238–46
[17] Jung S C and Han Y K 2013 How do Li atoms pass through the Al2O3 coating layer during lithiation in Li-ion batteries? *J. Phys. Chem. Lett.* **4** 2681–5
[18] Um N and Hirato T 2013 Dissolution behavior of La2O3, Pr2O3, Nd2O3, CaO and Al2O3 in sulfuric acid solutions and study of cerium recovery from rare earth polishing powder waste via two-stage *Mater. Trans.* **54** 713–9
[19] Rayzman V L, Aturin A V., Pevzner I Z, Sizyakov V M, Ni L P and Filipovich I K 2003 Extracting silica and alumina from low-grade bauxite *JOM* **55** 47–50
[20] Stanford Advance Materials 2021 ALF1461 aluminum alloy 1050 foil *samaterials*
[21] Signi Aluminium 2021 Aluminium foil alloy 1060 - 1060 aluminium foil *aluminium-foil.net*

[22] Targray 2021 Aluminium foil product data sheet *targray*
[23] Harris D C 2010 Standard reduction potential *Quantitative Chemical Analysis* (W. H. Freeman and Compan) pp AP20–7
[24] Nan J, Han D and Zuo X 2005 Recovery of metal values from spent lithium-ion batteries with chemical deposition and solvent extraction *J. Power Sources* **152** 278–84
[25] Meshram P, Abhilash, Pandey B D, Mankhand T R and Deveci H 2016 Acid baking of spent lithium ion batteries for selective recovery of major metals: A two-step process *J. Ind. Eng. Chem.* **43** 117–26
[26] Porvali A, Chernyaev A, Shukla S and Lundström M 2020 Lithium ion battery active material dissolution kinetics in Fe(II)/Fe(III) catalyzed Cu-H2SO4 leaching system *Sep. Purif. Technol.* **236** 116305
[27] Antolini E 2004 LiCoO2: Formation, structure, lithium and oxygen nonstoichiometry, electrochemical behaviour and transport properties *Solid State Ionics* **170** 159–71
[28] Julien C, Mauger A, Vijh A and Zaghib K 2015 *Lithium Batteries: Science and Technology*
[29] Dai T, Zhou H, Liu Y, Cao R, Zhan J, Liu L and Jang B W-L 2019 Synergy of lithium, cobalt, and oxygen vacancies in lithium cobalt oxide for airborne benzene oxidation: a concept of reusing electronic wastes for air pollutant removal *ACS Sustain. Chem. Eng.* **7** 5072–81
[30] Dorella G and Mansur M B 2007 A study of the separation of cobalt from spent Li-ion battery residues *J. Power Sources* **170** 210–5
[31] Basch A, De Campo L, Albering J H and White J W 2014 Chemical delithiation and exfoliation of LixCoO2 *J. Solid State Chem.* **220** 102–10
[32] Amalia D, Mubarok Z and Husaini 2014 Kinetics analysis for aluminum dissolution of West Kalimantan bauxite through digestion process *Indones. Min. J.* **17** 98–112
[33] Halliday J S 1954 The anodic behaviour of copper in caustic soda solutions *Trans. Faraday Soc.* **50** 171
[34] Joulié M, Billy E, Laucournet R and Meyer D 2017 Current collectors as reducing agent to dissolve active materials of positive electrodes from Li-ion battery wastes *Hydrometallurgy* **169** 426–32
[35] Awanis Hashim N, Liu Y and Li K 2011 Stability of PVDF hollow fibre membranes in sodium hydroxide aqueous solution *Chem. Eng. Sci.* **66** 1565–75
[36] Hausbrand R, Cherkashinin G, Ehrenberg H, Gröting M, Albe K, Hess C and Jaegermann W 2015 Fundamental degradation mechanisms of layered oxide Li-ion battery cathode materials: methodology, insights and novel approaches *Mater. Sci. Eng. B* **192** 3–25
[37] Li J, Lin C, Weng M, Qiu Y, Chen P, Yang K, Huang W, Hong Y, Li J, Zhang M, Dong C, Zhao W, Xu Z, Wang X, Xu K, Sun J and Pan F 2021 Structural origin of the high-voltage instability of lithium cobalt oxide *Nat. Nanotechnol.* **16** 599–605
[38] Xiong F, Yan H J, Chen Y, Xu B, Le J X and Ouyang C Y 2012 The atomic and electronic structure changes upon delithiation of LiCoO2: From first principles calculations *Int. J. Electrochem. Sci.* **7** 9390–400

Acknowledgements

The authors wish to acknowledge Total Green Recycling for supplying the spent laptop batteries used in this study. We also want to thank the laboratory technical support staff of Murdoch University for instrument training and technical assistance. D. Amalia wishes to acknowledge Australia Awards for the financial support in the form of a scholarship.